Modeling and Observing the Optical Thickness of Low Clouds

A. D. Del Genio, M.-S. Yao, W. Kovari, and A. B. Wolf
National Aeronautics and Space Administration
Goddard Institute for Space Studies
New York, New York

Introduction

A substantial portion of the disagreement in cloud feedback among various general circulation models (GCMs) can be traced to the models' differing representations of the optical thickness of low-level clouds. Implicit cloud optical thickness feedback arises when the optical properties are prescribed as a function of height, because cloud height typically increases in model simulations of a warming climate. If the optical thickness decreases with height, a positive low cloud optics feedback results. Diagnostic parameterizations, in which optical thickness is assumed to increase with temperature based on, e.g., a calculation of the adiabatic liquid water content of a moist lifted air parcel, produce a negative cloud optics feedback because the albedo effect dominates the greenhouse effect for low-level clouds. Prognostic schemes, in which cloud liquid/ice water is predicted as a function of time based on a cloud water budget and the optical properties diagnosed from the cloud water content, can produce either positive, neutral, or negative cloud optics feedbacks because such schemes incorporate both sources and sinks of cloud water.

To date, no observational or theoretical consensus has emerged on the temperature dependence of the optical thickness of low clouds. Aircraft observations compiled by Feigelson (1978) over the former Soviet Union indicate that the liquid water content of low and middle clouds increases with temperature except perhaps at the warmest temperatures. Somerville and Remer (1984) used this indication as the basis of an optical thickness feedback simulation in a one-dimensional radiative-convective (1DRC) model, illustrating the potentially large negative cloud optics feedback. Betts and Harshvardhan (1987) used simple thermodynamic arguments to calculate the temperature dependence of adiabatic liquid water content, with similar implications for low cloud optical thickness feedback. Curry et al. (1990), however, found no obvious liquid water path dependence on temperature in satellite microwave measurements over the North Atlantic.

More recently, Tselioudis et al. (1992) analyzed data from the International Satellite Cloud Climatology Project (ISCCP) relative to the temperature dependence of low cloud optical thickness associated with latitudinal, seasonal, and synoptic time scale variations. They found that over cold land areas, optical thickness does indeed increase with temperature, consistent with Feigelson's aircraft data. But over warm land areas and most ocean regions, where in situ data are almost nonexistent, optical thickness tends to decrease with temperature instead. If this is indicative of the low cloud component of optical thickness feedback in a warming climate, there are major implications for climate sensitivity and the polar amplification of warming (Tselioudis et al. 1993).

The goal of this Atmospheric Radiation Measurement (ARM) research is to explore the causes of the counter-intuitive ISCCP result, using a combination of ARM data and single-column modeling. For example, the ISCCP data alias subpixel fractional cloudiness into an underestimate of optical thickness that is due to a relatively coarse pixel size. If this bias is a systematic function of temperature (e.g., stratus giving way to shallow cumulus as temperature rises), the implied optical thickness feedback might be a cloud cover effect instead.

On the other hand, the ISCCP result may be real and indicative of either temperature-dependent cloud water sinks (precipitation, entrainment), cloud physical thickness variations, or droplet effective radius variations. The ARM data set can help us constrain the possible explanations because it will enable us to 1) examine a variety of cloud properties on scales smaller than an ISCCP pixel and 2) test hypotheses on low cloud optics feedback

mechanisms with a single-column version of a GCM cloud parameterization forced with actual dynamical and surface fluxes. Preliminary work in these areas is described below.

Validation of Goddard Institute for Space Studies GCM Cloud Properties Against ISCCP Data

We are currently developing a prognostic cloud liquid/ice water budget parameterization for the Goddard Institute for Space Studies (GISS) GCM (Del Genio et al. 1993). Cloud formation in the scheme follows the approach of Sundqvist et al. (1989), but sources and sinks of cloud water and representations of optical properties are unique to the GISS scheme.

The model parameterizes all important cloud microphysical processes, including autoconversion, accretion of cloud water by rain, Bergeron-Findeisen diffusional growth of ice in a mixed phase cloud, and evaporation of cloud water and precipitation. Small scale dynamical sources (detrainment of cumulus condensate into anvils) and sinks (cloud top entrainment instability, using a very restrictive criterion) are also included.

Interactive visible cloud optical thickness is based on the predicted cloud water content and a diagnosis of droplet effective radius, assuming constant number concentration (different for land and ocean clouds, and for liquid and ice). Particle size increases only up to the threshold for efficient precipitation formation, itself also different for land and ocean and for liquid and ice. The spectral dependence is calculated from Mie theory, guaranteeing self-consistent shortwave and longwave cloud radiative properties. Ice clouds are treated as equivalent spheres.

Validation of GCM cloud parameterizations often involves simple comparisons with top-of-the-atmosphere (TOA) radiative fluxes and/or total cloud cover. However, these quantities integrate the effects of many cloud types and thus are not unique indicators of the validity of a cloud parameterization. Consider, for example, the January TOA absorbed solar flux observed (during the Earth Radiation Budget Experiment [ERBE]) and simulated at the first three ARM sites:

	TOA Solar Flux (W/m^2)	
	ERBE	GCM
Southern Great Plains	129	120
Tropical West Pacific		
147°E, 3°S	309	302
174°E, 2°N	303	300

The good agreement between model and data suggests a successful parameterization, but might instead be the result of compensating errors in different cloud types or in cloud cover and optical thickness. Since different clouds have different feedback effects in a climate change, it is important to validate the simulation of specific cloud types. In practice, validation is difficult for several reasons: 1) Current satellite instruments detect only the highest cloud top and the column-integrated optical thickness rather than the properties of each individual cloud; 2) very thin clouds may be missed or their top pressure misidentified in satellite data; 3) satellite optical thicknesses are biased downward by subpixel fractional cloudiness; 4) GCM errors in cloud simulation can be due to errors in dynamical and/or surface fluxes of heat and moisture rather than to deficiencies in the cloud scheme itself.

To account for the first two problems, we view the GCM as the satellite would see it. We diagnose only the highest cloud top and the column optical thickness at each timestep in each GCM gridbox. Furthermore, we mimic ISCCP's misidentification of very optically thin clouds using guidelines based on comparisons of nearly coincident ISCCP and SAGE II (Stratospheric Aerosol and Gas Experiment) data (Liao et al., in press). Briefly, in this approach, we ignore the highest clouds whose optical thickness $\tau < 0.1$, placing clouds with $0.1 < \tau < 0.3$ at the tropopause, and placing the cloud tops of clouds with $0.3 < \tau < 0.5$ one model level (approximately 100 mb) lower than the actual cloud top.

Figure 1 shows the GISS GCM simulated frequency distribution of "satellite-observed" cloud top pressure and optical thickness for the grid boxes which include the ARM Southern Great Plains (SGP), Tropical West Pacific (TWP), and North Slope of Alaska sites, as well as the ISCCP-detected cloud type distribution for the same locations, for the month of January. (There is no ISCCP plot for the North Slope, which is mostly in darkness in January and thus contains no optical thickness information.)

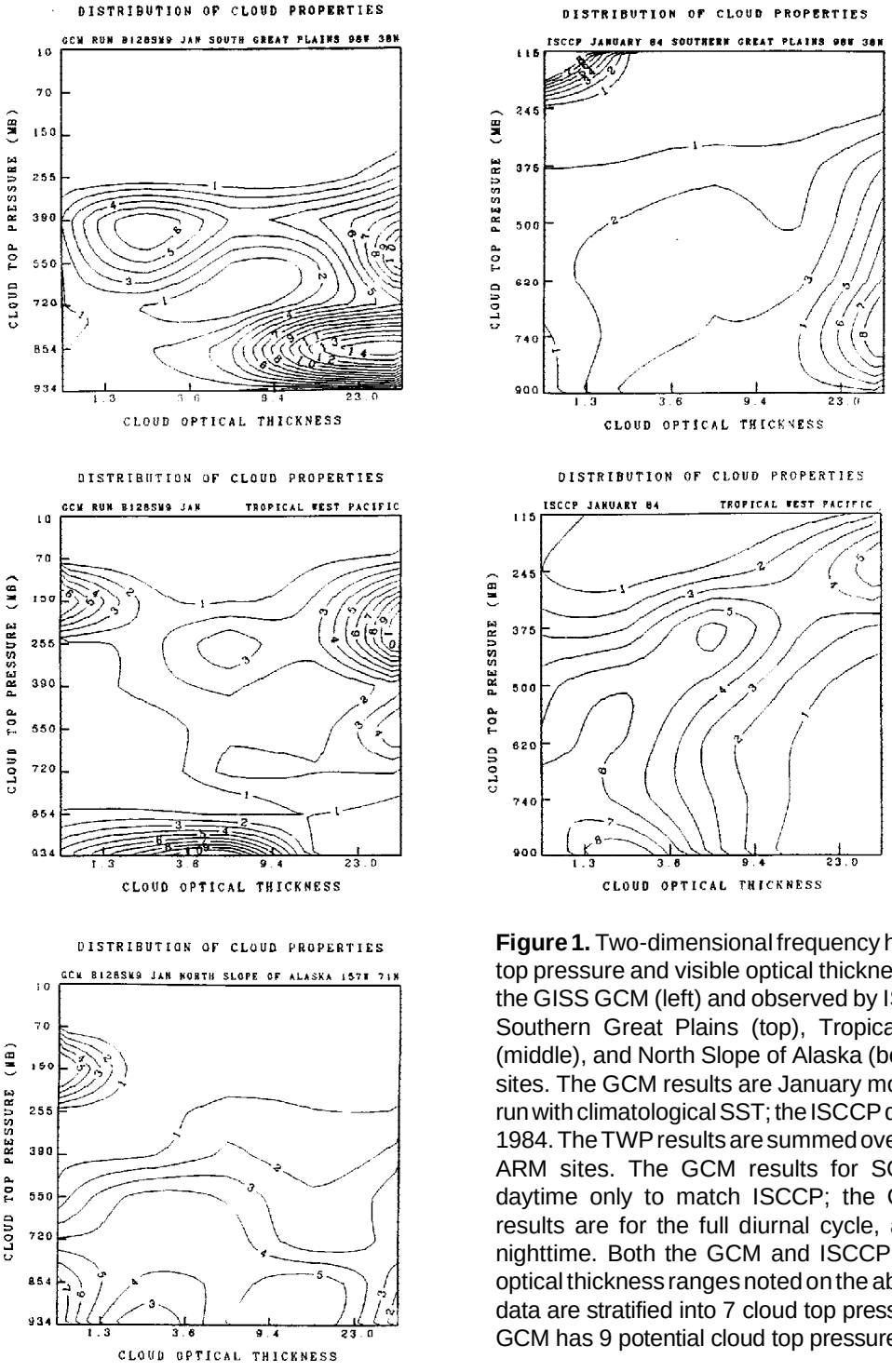

Figure 1. Two-dimensional frequency histograms of cloud top pressure and visible optical thickness as simulated by the GISS GCM (left) and observed by ISCCP (right) at the Southern Great Plains (top), Tropical Western Pacific (middle), and North Slope of Alaska (bottom) ARM CART sites. The GCM results are January monthly totals from a run with climatological SST; the ISCCP data are for January 1984. The TWP results are summed over the two proposed ARM sites. The GCM results for SGP and TWP are daytime only to match ISCCP; the GCM North Slope results are for the full diurnal cycle, almost exclusively nighttime. Both the GCM and ISCCP are binned into 5 optical thickness ranges noted on the abscissa. The ISCCP data are stratified into 7 cloud top pressure bins, while the GCM has 9 potential cloud top pressure levels.

The dominant January cloud types at the SGP site are optically thick stratus and nimbostratus with cloud tops mostly at 600-800 mb. The GCM also preferentially produces low and mid-level optically thick clouds, but over a somewhat larger range of altitudes and with a minimum near 700 mb not seen in ISCCP.

The ISCCP data also indicate a secondary broad maximum of mid-level clouds of low to moderate optical thickness. The GCM simulates this maximum as well, but about 100 mb higher and somewhat optically thinner than in the data.

A third ISCCP maximum of thin high cirrus (misplaced by the ISCCP algorithm) is not simulated by the GCM. In this and other regions, the GCM's clouds are more concentrated in a few cloud types than is true of the real world. There are two reasons for this: the GCM's radiation code selects a single cloud type at any instant for a 4°x5° gridbox, while an ISCCP 2.5°x2.5° cell contains multiple cloud types at any instant. In addition, four ISCCP cells are added to produce an area comparable to that of a single GCM gridbox, thus allowing for more variability than the GCM is capable of producing.

At the TWP sites, ISCCP indicates a maximum in very low-level (900 mb), fairly optically thin stratus clouds, but with a significant fraction of these clouds extending as high as 550 mb. Also present are secondary maxima that are due to deep cumulonimbus and slightly less deep thick cirrus. The GCM simulates a 900-mb maximum as well, but with optical thicknesses in the next highest ISCCP category. A primary goal of our ARM research will be to understand whether this discrepancy is real, and if so, the physical mechanisms which cause the GCM to overestimate low cloud optical thickness in the tropics. This difference is at the heart of the low cloud optical thickness feedback question. At high altitude, the GCM correctly simulates both the deep cumulonimbus and the thick cirrus peaks, although it places the latter about 100 mb higher in altitude than ISCCP indicates. The GCM also produces a thin cirrus population not seen by ISCCP.

At the North Slope of Alaska site, the GCM produces both very thin and optically thick concentrations of low clouds with tops at 850-900 mb and a weak secondary maximum of moderate optical thickness clouds with 600-800 mb tops. There are no ISCCP optical thickness data for this site, which is in darkness in January. We note, however, that near the summer pole, ISCCP detects clouds that are systematically optically thicker than those simulated by the GCM. Whether this is a model deficiency or the result of the difficulty that ISCCP experiences in cloud detection over snow/ice covered surfaces is not clear. In situ data from the planned ARM Cloud and Radiation Testbed (CART) site in Alaska will be helpful in diagnosing GCM performance in this region.

Overall the GCM results are encouraging, but it is difficult to know how much impact (negative or positive) the GCM's large-scale dynamics deficiencies have on the cloud parameterization's performance. It is clear, for example, that the GCM's midlatitude eddy kinetic energy is underestimated, and this underestimate can be expected to affect the heat and water vapor transports that control midlatitude cloud formation. Testing the parameterization in single-column model mode, forced by observed dynamical and surface fluxes at the CART sites, will yield a more definitive evaluation of the cloud scheme's capabilities.

Liquid Water Observations at the Southern Great Plains Site

To understand optical thickness variations, we need to understand variability in the liquid water content of low-level clouds. Data from the Microwave Water Radiometer (MWR), operated by J. Liljegren, are already available at the SGP CART site. The standard MWR product is the column liquid water path at 5-minute resolution, with estimated 10% accuracy and 1% precision. For a 5-10 m/s horizontal wind speed, the corresponding effective spatial resolution is 1.5-3.0 km, somewhat better than that of an ISCCP pixel. Higher resolution estimates are also available, albeit with lower precision.

As a first step in the analysis of low cloud optical thickness variations, we are studying seasonal variations of liquid water path at the SGP site. Figure 2 shows histograms of MWR liquid water path measurements for a cold month (November 1992) and a warm month (June 1993).

Quality control flags have been used to eliminate outliers in the data. Nonetheless, the measurements suggest that some bad data remain. Above liquid water paths of approximately 0.08 cm, the distribution of liquid water does

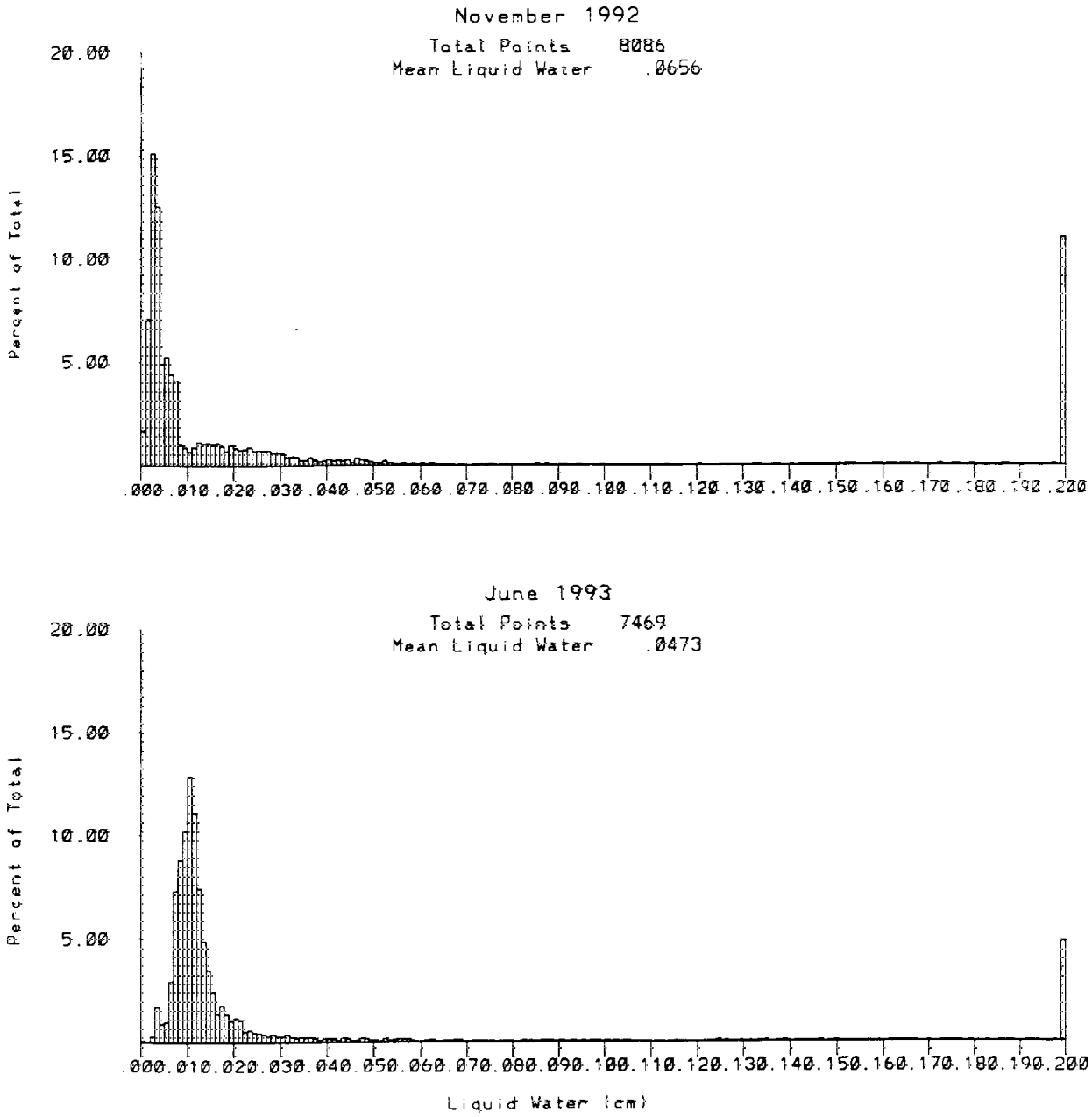

Figure 2. Histograms of MWR liquid water path (5-minute averages) at the SGP site for November 1992 (top) and June 1993 (bottom). All data are included except those identified by the quality flags. All points >0.20 cm are grouped into the last bin.

not approach zero but resembles white noise instead. This value is close to the upper limit seen by satellite microwave radiometers and corresponds to an optical thickness τ = 120 for a 10 μm effective radius, about the maximum that can be distinguished in visible radiance data such as ISCCP.

We therefore eliminate all liquid water path data which exceed 0.08 cm (Figure 3); the precise value of the cutoff does not matter, but the existence of a cutoff somewhere in the distribution does.

Without any high-end cutoff, the mean liquid water path (averaged over all nonzero liquid water occurrences) is greater in November (0.0656 cm) than in June (0.0473 cm), consistent with the ISCCP optical thickness results if taken at face value. However, if liquid water paths > 0.08 cm are excluded, the mean liquid water path is greater in June (0.0133 cm) than in November (0.0114 cm).

Interpreting these results at this stage is difficult since the data include all clouds and therefore, seasonal variations in physical thickness, which may be substantial, are convolved with liquid water content variations in Figure 3. In addition, dynamics and aerosol influences have not yet been taken into account.

Even so, the preliminary results suggest that if, for the sake of discussion, the liquid water path variation is attributed strictly to liquid water content variation, then the implied temperature dependence is much weaker (1% per °C) than would be characteristic of adiabatic liquid water contents. The results also suggest that the November distribution has a longer tail than that in June, i.e., more high liquid water events, despite the fact that the vertical extent of liquid water in November is limited by the lower freezing level. For a more definitive assessment, we will require coincident cloud top, cloud base, vertical velocity, and aerosol data to isolate the actual temperature dependence for low level clouds.

References

Betts, A. K., and Harshvardhan. 1987. Thermodynamic constraint on the cloud liquid water feedback in climate models. *J. Geophys. Res.* **92**:8483-8485.

Curry, J. A., C. D. Ardeel, and L. Tian. 1990. Liquid water content and precipitation characteristics of stratiform clouds as inferred from satellite microwave measurements. *J. Geophys. Res.* **95**:16659-16671.

Del Genio, A. D., M.-S. Yao, and C. E. Wendell. 1993. GCM feedback sensitivity to interactive cloud water budget parameterization. Preprints, *4th Symposium on Global Change Studies*, pp. 176-181. American Meteorological Society, Boston, Massachusetts.

Feigelson, E. M. 1978. Preliminary radiation model of a cloudy atmosphere. Part I - Structure of clouds and solar radiation. *Beitr. Phys. Atmos.* **51**:203-229.

Liao, X., D. Rind, and W. B. Rossow. Comparison between SAGE II and ISCCP high-level clouds. Part II: Cloud vertical structures. *J. Geophys. Res.*, in press.

Somerville, R.C.J., and L. A. Remer. 1984. Cloud optical thickness feedbacks in the $C0_2$ climate problem. *J. Geophys. Res.* **89**:9668-9672.

Sundqvist, H., E. Berge, and J. E. Kristjánsson. 1989. Condensation and cloud parameterization studies with a mesoscale numerical weather prediction model. *Mon. Wea. Rev.* **117**:1641-1657.

Tselioudis, G., W. B. Rossow, and D. Rind. 1992. Global patterns of cloud optical thickness variation with temperature. *J. Clim.* **5**:1484-1495.

Tselioudis, G., A. A. Lacis, D. Rind, and W. B. Rossow. 1993. Potential effects of cloud optical thickness on climate warming. *Nature* **366**:670-672.

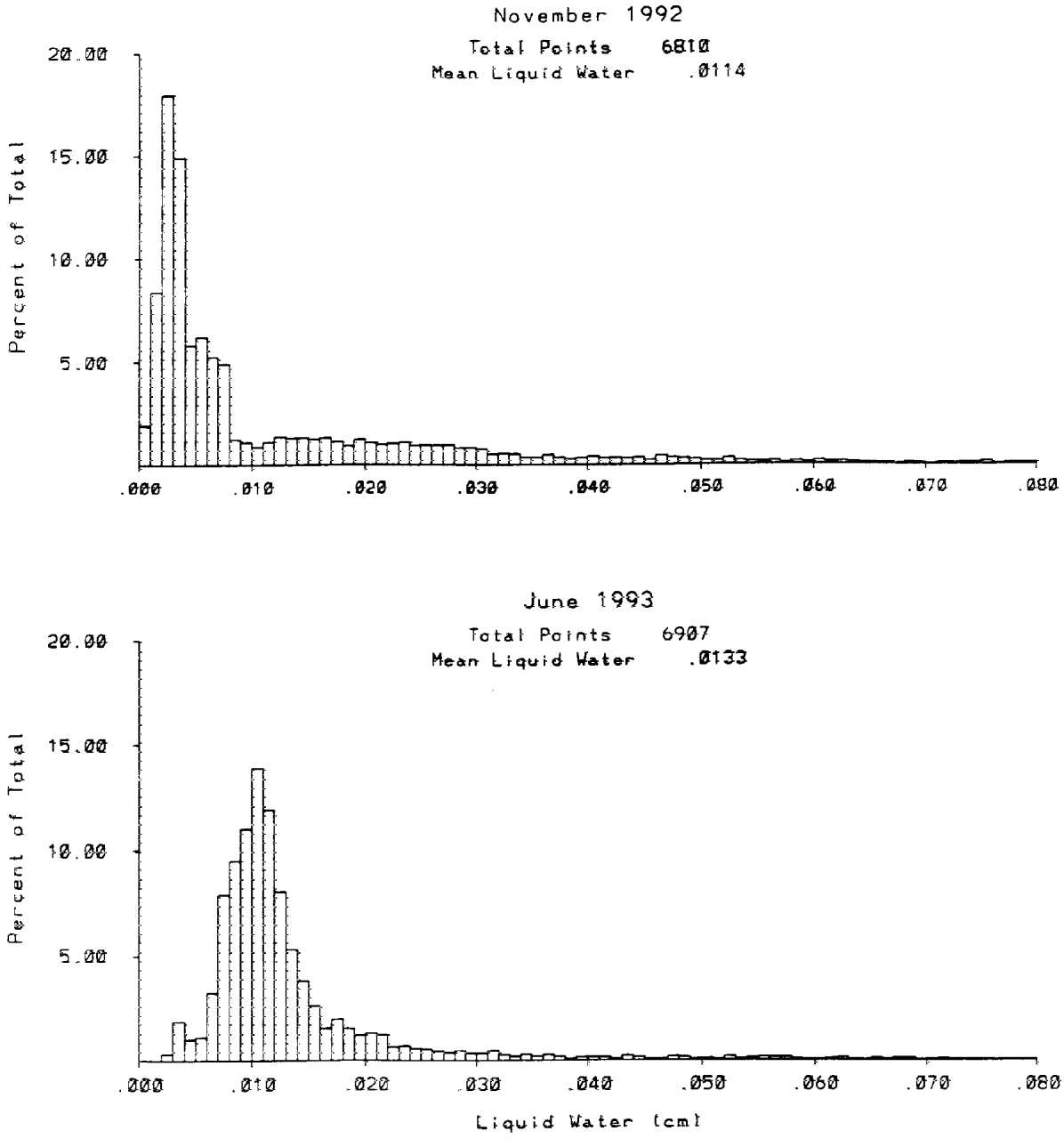

Figure 3. As in Figure 2 but excluding liquid water path points >0.08 cm.